

Mouse Knee Spatial Transcriptomics Reveals Injury Programs Associated with the Infrapatellar Fat Pad in Aging

David Carro Vazquez^{1*}, Tiffany G. Lam^{2*}, Tiffany T. K. Pham¹, Hope D. Welhaven¹, Tamara Alliston³, Allon Wagner^{2†}, Kelsey H. Collins^{1†}

¹University of California, San Francisco, CA, ²University of California, Berkeley, CA, ³NIAMS Intramural Research, NIH

*equal contribution, †equal contribution, [Email: tiffany.pham2@ucsf.edu](mailto:tiffany.pham2@ucsf.edu)

Disclosures: None

INTRODUCTION: Osteoarthritis (OA) is a leading cause of pain and disability worldwide. Single-cell spatial information is required to resolve tissue-specific changes in whole-knee joint tissues and to decode the mechanisms of aging and injury in the joint organ system. However, the extracellular matrix-rich joint tissues have been resistant to the applications of spatial-omics approaches¹. To meet this need, our lab has developed spatial transcriptomics approaches in formalin-fixed paraffin-embedded knee joints in collaboration with 10x Genomics. In this study, we leverage data from adult and aged joint tissues challenged with destabilization of the medial meniscus, sham, or no surgery to determine if injury is an accelerated aging process in the knee joint. We **hypothesized** that transcriptomic changes in the infrapatellar fat pad (IPFP) with aging are distinct from those that occur with injury.

METHODS: Male mice were challenged with either destabilization of the medial meniscus (DMM), sham, or no surgery as adults (4 months of age) and euthanized at 7 months. Aged mice were challenged with surgery at 6 months of age and euthanized at 24 months of age (n = 5 – 10/group). Whole knee joints were fixed in 4% PFA, decalcified in 10% formic acid, and processed for formalin-fixed paraffin-embedded histology. Histological sections were assessed for OA severity using Modified Mankin Score and whole knee joints were prepared according to the Visium HD Kit (10x Genomics) for spatial transcriptomics in the sagittal plane (n = 2/group). Slides were processed by Space Ranger v3.0.1 (10x Genomics), and molecule misassignment was mitigated by ResoLVI². A low-dimensional representation of barcode transcriptomes was computed with ResoLVI and clustered with the Leiden algorithm. Tissues were expertly segmented and validated using tissue-specific marker genes from publicly available datasets^{3,4,5}. Unbiased spatial segmentation of the joint into cell neighborhoods was performed with NOLAN⁶.

RESULTS: Modified Mankin Score was increased in adult DMM compared to adult naïve joints, and further increased in aged DMM compared to both aged naïve and adult DMM joints, indicating that the aging milieu exacerbated joint injury (Fig. 1B-C). To define the aging signature, we compared naïve whole knee joints between aged and adult groups to identify differentially expressed genes (Fig. 1D). *Coll1a1*, which is reported to increase in osteoarthritic bone⁶, was upregulated in aged naïve joints compared to adult naïve joints. When we compared differential gene expression between aged naïve and adult DMM-injured joints (Fig. 1E-F), we also observed increases in *Coll1a1* and several downregulated genes, including *Igkc*, *Pf4*, *Pppbp*, concordant with similar Modified Mankin Scores between the groups. *Htral* and *Spp1* were uniquely upregulated in adult DMM joints compared to adult sham. In aged DMM animals, gene set enrichment analysis revealed downregulation of lipid biosynthesis, oxidative phosphorylation, and mitochondrial ATP synthesis, suggesting reduced cellular energy production compared to adult DMM. Finally, despite increased Mankin Scores in aged sham and aged DMM joints compared to aged naïve, each injury induced a distinct transcriptional signature revealing opposing regulatory patterns (Fig. 1G). The IPFP (Fig. 2A-B) was transcriptionally distinct from the synovium, including transcripts for *Scd1*, and *Cfd*. We leveraged NOLAN (No-Label Analysis of Niches), a self-supervised deep-learning framework, to combine single-cell gene expression with spatial neighborhood information and to define distinct cellular neighborhoods and gradual transitions between them (Fig. 2C, D, E). Notably, we observed two distinct IPFP niches, one of which was markedly enriched with DMM, and defined by upregulation of *Coll1a1*, *Coll1a2*, and *Sparc* compared to naïve or sham. This niche occurred in both adult and aged joints, suggesting it represents an injury-associated microenvironment, which was observed in spatial proximity to the synovium node. The second niche, which represents a potential aging IPFP niche, is defined by upregulation of *Scd1*, *Cfd*, and *Fabp4*.

DISCUSSION: Injury-induced OA by DMM is not simply accelerating age-related processes. We leverage single-cell resolution spatial transcriptomics to demonstrate that aging and injury create distinct molecular landscapes in joint tissues, challenging the long-held notion that OA is an inevitable consequence of aging. While injury can partially phenocopy aging, as indicated by the shared molecular changes in both aged naïve and adult DMM joints, this mimicry is selective and tissue dependent. The opposing transcriptional signatures observed in aged sham compared to aged DMM joints highlight that similar histological damage can arise from different – and in this instance opposite – molecular mechanisms, highlighting the need for high-dimensional spatial data to define molecular mechanisms and tissue-specific changes driving OA. Beyond emphasizing disease complexity, this opposition highlights a critical methodological consideration: in the context of a vulnerable joint, such as with aging, sham surgery may not serve as an appropriate surgical control as it drives a unique injury-like molecular signature. As expected, we observed transcriptomic nodes with aging that are separable. Additionally, while many studies have focused primarily on pathogenic changes in cartilage, our data suggest that the changes in other joint tissues, like the IPFP, are more overt than those detected in cartilage – but that might be due to cartilage loss and low cellularity compared to the IPFP. As such, there is an opportunity to leverage sophisticated molecular tools to resolve mechanistic changes that are beyond the scope of typical histology that cannot be targeted using other genetic tools. Our ongoing work is integrating dissociative single-cell sequencing to improve sequencing depth in this dataset and further probe tissue-specific changes with sex, aging, and injury. Importantly, our spatial niche analysis identifies the IPFP as both an injury and aging microenvironment, which aligns with our prior work demonstrating fat-cartilage crosstalk as a driver of OA. Moreover, consistent with our previous spatial transcriptomics work, we identify *Cfd* as a key marker of the IPFP using first-generation Visium. We and others have previously demonstrated *Cfd* plays a role in cartilage damage and pain¹. We posit that these data position the IPFP as a transducer of interorgan crosstalk between the joint and the organism. These findings build upon our previous observations that systemic adipose drives knee OA⁷ and suggest that it is important to consider both *how* systemic adipose communicates with the joint and *how* intra-articular adipose contributes to local pathology – and critically, whether these fat depots communicate *with each other* to amplify disease burden.

SIGNIFICANCE/CLINICAL RELEVANCE: Spatial -omics can be used to define the aging and injury signature across the lifespan in mice, especially to capture the spatial tissue-specific transcriptional states in the IPFP that have been difficult to define in translational OA models. Age-related OA and DMM-induced pathology involve distinct molecular mechanisms that appear to drive divergent molecular patterns and pathology. These data will allow us to target and to define precise tissue-joint crosstalk mechanisms and to decode novel pathways for OA treatment unlocked by advancements in spatial biology.

REFERENCES ¹Collins+ Sci Adv 2025, ²Ergen+ BioRxiv 2025, ³Tabula Muris+ Nature 2020, ⁴Han+ Cell 2018, ⁵Harasymowicz+ Ann Rheum Dis 2025; ⁶Bakulin+ ICLR 2025; ⁷Truong+ Arthritis Res Ther 2006; ⁸Collins+ PNAS 2021

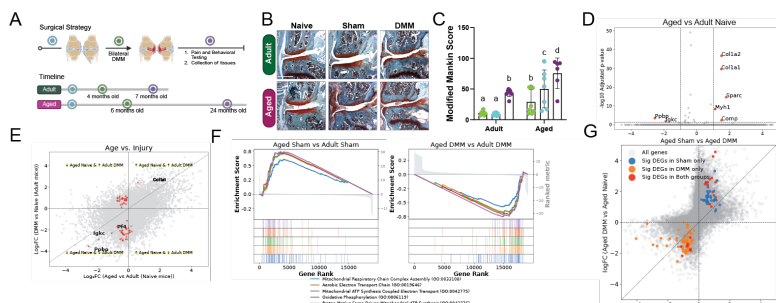


Figure 1. (A) Surgical methods and age groups. (B) Medial Saf-O/Fast Green histological sections (scale bar = 400 μm). (C) Modified Mankin Score. (D) Volcano plot of differentially expressed genes (DEGs) between aged and adult naïve mice (red = significant by BH-adjusted $p < 0.05$). (E) Log fold-change (logFC) of DEGs with aged vs. adult naïve on x-axis and DMM vs. naïve in adult mice on y-axis. (F) Gene set enrichment analysis against GO Biological Processes of aged Sham and aged DMM. (G) Scatterplot of DEG with aged sham vs. aged naïve on x-axis and aged DMM vs. aged naïve on y-axis, similar to E (blue = significant in sham only, orange = significant in DMM only, red = significant in both).

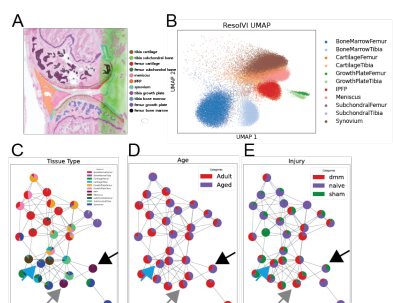


Figure 2. (A) Visium HD spatial transcriptomics with tissue annotation (B) UMAP of whole transcriptomes (C-E) NOLAN unbiasedly infers shared spatial niches across samples (nodes). Spatially proximal niches are connected by edges. Grey arrow indicates a DMM-associated IPFP niche, and the black arrow a second IPFP niche. Blue arrow indicates a synovial niche proximal to the DMM-associated, but not to the other, IPFP niche.